Article

Not peer-reviewed version

The Distal Promoter of the *B438L* Gene of African Swine Fever Virus Is Responsible for the mRNA Transcription of the *B438L* and the Alternatively Spliced *B169L*

Hongwei Cao , Hao Deng , Yanjin Wang , Diqiu Liu , Lian-Feng Li , Meilin Li , Dingkun Peng , Jingwen Dai , Jiaqi Li , Hua-Ji Qiu * , Su Li *

Posted Date: 3 May 2024

doi: 10.20944/preprints202405.0180.v1

Keywords: African swine fever virus; *B438L* promoter; transcription initiation; B169L protein

 doi:10.20944/preprints202405.0180.v1

Article

The Distal Promoter of the *B438L* Gene of African Swine Fever Virus Is Responsible for the mRNA Transcription of the *B438L* and the Alternatively Spliced *B169L*

Hongwei Cao †, Hao Deng †, Yanjin Wang, Diqiu Liu, Lian-Feng Li, Meilin Li, Dingkun Peng, Jingwen Dai, Jiaqi Li, Hua-Ji Qiu * and Su Li *

State Key Laboratory for Animal Disease Prevention and Control, National African Swine Fever Para-Reference Laboratory, National High-Containment Facilities for Animal Disease Control and Prevention, Harbin Veterinary Research Institute, Chinese Academy of Agricultural Sciences, Harbin, China; chw18344306620@163.com (H.C.); denghao333417@163.com (H.D.); wangyanjin1996@126.com（Y.W.）; liudiqiu@caas.cn (D.L.); lilianfeng@caas.cn(L.L.); m18037901611@163.com (M.L.); pengdk11@163.com (D.P.); dai_wener@163.com (J.D.); lijiaqi1051951442@163.com(J.L.)

* Correspondence: Hua-Ji Qiu (H.Q.): qiuhuaji@caas.cn; Su Li: lisu@caas.cn(S.L.)

Abstract: The B169L protein (pB169L) of African swine fever virus (ASFV) is a structural protein with an unidentified function during the virus replication. The sequences of the *B169L* gene and the downstream *B438L* gene are separated by short intergenic regions. However, the regulatory mode of the gene transcription remains unknown. Here, we identified two distinct promoter regions and two transcription start sites (TSS) located upstream of the open reading frame (ORF) of *B438L*. Using the promoter reporter system, we demonstrated that the cis activity of the ORF proximal promoter exhibited significantly higher levels compared with that of the distal promoter located in the *B169L* gene. Furthermore, transfection with the plasmids with two different promoters for *B438L* could initiate the transcription and expression of the *B438L* gene in HEK293T cells, and the cis activity of the ORF proximal promoter also displayed the higher activities compared with the distal promoter. Interestingly, the *B438L* distal promoter also initiated the transcription of the alternatively spliced *B169L* mRNA (*B169L* mRNA2) encoding a truncated pB169L (tpB169L) (amino acids 92–169), and the gene transcription efficiency was increased upon mutation of the initiation codon located upstream of the alternatively spliced *B169L* gene. Taken together, we demonstrated that the distal promoter of *B438L* gene initiates the transcription of both the *B438L* mRNA and *B169L* mRNA2. Comprehensive analysis of the transcriptional regulatory mode of the *B438L* gene is beneficial for the understanding of the association of B438L protein and pB169L and the construction of the gene-deleted ASFV.

Keywords: African swine fever virus; *B438L* promoter; transcription initiation; B169L protein

1. Introduction

African swine fever (ASF), caused by African swine fever virus (ASFV), is a highly contagious and hemorrhagic disease of swine with high mortality up to 100% [1]. Since its initial outbreak in Kenya in the 1920s, ASF had predominantly manifested as an epidemic in Europe, South America and the Caribbean [2]. However, the disease was introduced into China in 2018 and resulted in huge economic losses due to the lack of effective vaccines and antiviral drugs [3,4]. ASFV belongs to the family *Asfarviridae* and is a large enveloped virus with a genome of double-stranded DNA, encoding more than 150 proteins [5]. However, the functional role of the structural protein B169L (pB169L) remains elusive. The open reading frame (ORF) of *B169L* comprises 495 base pairs (bp) and is translated into pB169L with 169 amino acids (aa). It is noteworthy that the transcription of *B169L* gives rise to two mRNAs: a full-length of *B169L* mRNA and an alternatively spliced *B169L* mRNA (referred to as *B169L* mRNA2) encoding a truncated pB169L (tpB169L) (aa 92–169) [6]. However, the

 doi:10.20944/preprints202405.0180.v1

TSS and the promoter responsible for the generation of *B169L* mRNA2 remain unknown. Notably, the *B169L* gene is arranged adjacent with its downstream gene *B438L* in the ASFV genome. Therefore, we postulated that the promoter sequence of the downstream gene *B438L* is located within the *B169L* gene.

A previous study has revealed that the ASFV B438L protein (pB438L) is indispensable for the construction of the icosahedral capsid of ASFV, and the gene-deletion of *B438L* leads to a significant alteration in virion assembly, resulting in the formation of tubular viral particles instead of the characteristic icosahedral capsid, thereby disrupting the icosahedral symmetry [7,8]. The morphological perturbation also affects the infectivity and pathogenicity of viruses. It has been shown that the transcriptional machinery of ASFV exhibits complexity, which is involved in the complex interplay between enzymes and cofactors encoded by ASFV [9]. The ORFs of ASFV *B438L* and *B169L* are densely distributed in an organized manner, it is possible that the upstream gene encompasses promoters to govern the expression of the downstream gene of ASFV, and an individual gene may harbor multiple promoters for the initiation of downstream viral gene transcription. Therefore, it is essential to decipher the transcriptional regulation patterns of the downstream *B438L* gene, which will facilitate the design of the *B169L*-deleted ASFV.

In this study, we have elucidated an intricate interrelationship between the ASFV *B438L* gene and its adjacent upstream and downstream genes. Notably, the *B438L* promoter region is located in the upstream of its ORF and encompasses two distinct promoters, and the *B438L* distal promoter also initiates the transcription of alternatively spliced *B169L* (*B169L*-2). Moreover, we have discerned that the transcriptional activity of the *B438L* gene depends on the viral transcriptional machinery, in conjunction with relevant cofactors, and the transcription efficiency of the gene was also affected by the ATG located upstream of *B169L-2*. The findings enhance our understanding of transcriptional mechanism underlying ASFV, thereby providing novel insights into the development of antiviral strategies.

2. Materials and Methods

2.1. Cells and Viruses

Primary porcine alveolar macrophages (PAMs) or HEK293T cells were cultured in RPMI 1640 or Dulbecco's modified Eagle's medium supplemented with 10% fetal bovine serum (FBS), 100 units/mL penicillin and 100 μg/mL streptomycin at 37°C with 5% CO_2. The ASFV HLJ/2018 strain was isolated from field pig samples in China and propagated in the PAMs as described previously [10].

2.2. 5' and 3' Rapid Amplification of cDNA Ends (RACE) Assay

The total RNA was extracted from the ASFV-infected PAMs at a multiplicity of infection (MOI) of 2 using an RNA purification kit (catalog no. BSC52M1; BioFlux) according to manufacturer's instructions. The 5′RACE was performed using the 5′-Full RACE kit (catalog no. 638858; TaKaRa) and the B438L-specific primers (B438L-GSP1 and -GSP2 primers). The schematic diagram of the B438L-GSP 1 and -GSP 2 for 5′RACE was shown in Figure 1. The gene products of 5′RACE polymerase chain reaction (PCR) were cloned into the pMD19-T vector (catalog no. 639648; TaKaRa) and sequenced using the M13 primers. All the primers in this study are shown in Table 1.

 doi:10.20944/preprints202405.0180.v1

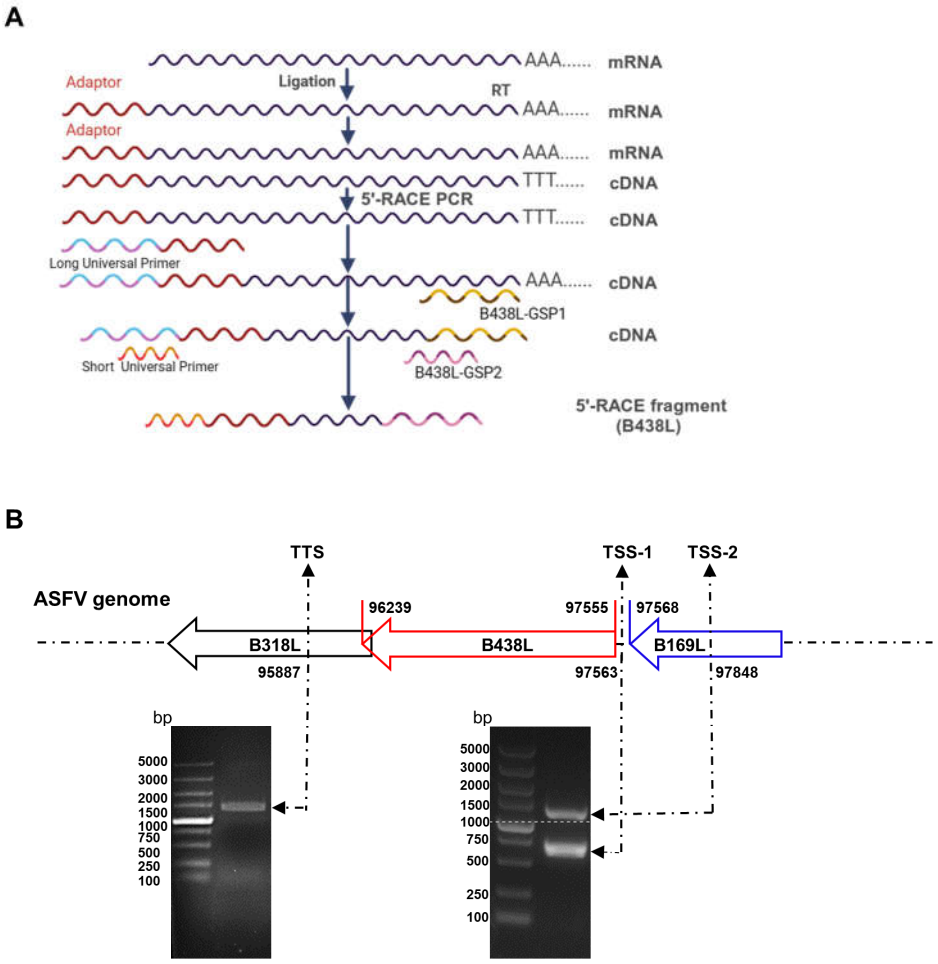

Figure 1. Two distinct initiation sites for the transcription of the *B438L* gene of African swine fever virus. (A) Preparation of cDNAs. Total RNA was obtained from the ASFV-infected PAMs at 24 hours postinfection, and cDNAs were synthesized using SMARTer RACE 5′/3′ kit. After removal of the 5′ phosphate groups and the 5′ cap structure by calf intestine alkaline phosphatase and Tumor Abnormal Protein, respectively, the adaptor was fused to the 5′-terminal end of the mRNA using T4 RNA ligase. RT, reverse transcription. (B) Identification of the *B438L* transcript. At the upper panel, the numbers represent the respective loci of the initiation codon ATG, stop codon TAGof the *B438L* in the genome of ASFV HLJ/2018 strain. The bottom panel shows that the PCR products were stained with ethidium bromide in a 1.2% agarose gel. The numbers on either side of the image indicate the corresponding sites of TSS-1 (lower band), TSS-2 (upper band), and the TTS in the ASFV genome. TSS, transcription start site; TTS, transcription termination site.

Table 1. The sequences of the primers used for PCR.

Primers	Sequences (5′–3′)	Description
Long Universal Primer	CTAATACGACTCACTATAGGGCAAGCAGTGGTATCAACGCAGAGT	B438L
Short Universal Primer	CTAATACGACTCACTATAGGGC	B438L
GSP1	GATTACGCCAAGCTTAGCATCGGCACGTCCGTGTAGGTAC	B438L
GSP2	GATTACGCCAAGCTTGTGTGCTCGCTGAACCTCGTAGAAG	B438L
B438L-1.F	CCGCTCGAGTGTATATAAAAGTTAATTATTATATTG	
B438L-1.R	GGGGTACCTGCGACTACATTAGCAATCTGGGCACC	B438L-1
B438L-2.F	GGGGTACCCCATTAGATAACTATCCCGTGCCAC	B438L-2
B438L-3.F	GGGGTACCAGTCGGGCCTTTTTGAAGAATCTTC	B438L-3
B438L-4.F	GGGGTACCTAGATTTTATTGCGGGTATCAATAA	B438L-4
B438L-5.F	GGGGTACCGCCCTATTATTTTTGCATTATTATG	B438L-5
B438L-6.F	GGGGTACCATAAGGGCGGAGATGAAATTATTCC	B438L-6
B438L-7.F	GGGGTACCTGCGACTACATTAGCAATCTGGGCACC	B438L-7
B438L-7.R	CCGCTCGAGTACAATGCATATATATACGTAAATAGC	

 doi:10.20944/preprints202405.0180.v1

B438L-5-mTA.F	CCTTCTCAAAACCAAAATAATTAAC	B438L-5-mTA
B438L-5-mTA.R	GTTAATTATTTTGGTTTTGAGAAGG	
B438L-5-mGC.F	ATTATGCCTTCTCAAAATTAACTTT	B438L-5-mGC
B438L-5-mGC.R	AAAGTTAATTTTGAGAAGGCATAAT	
B438L-7-dGC.F	AATGTAGATTTTATTATCAATAATTTAGGA	B438L-7-dGC.
B438L-7-d.GC.R	TCCTAAATTATTGATAATAAAATCTACATT	
pMD-Flag-B438L-I.F	CGGATCCTATAATAAATCAAACATGGATGTA	pMD-Flag-B438L-I
pMD-Flag-B438L-I.R	TAAGAACTACTTATCGTCGTCATCCTTGTAATCCAATGATGGAGATATA GATG	
pMD-Flag-B438L-II.1F	CGGATCCGTCGGGCCTTTTTGAAGAATCTTCA	pMD-Flag-B438L-II
pMD-Flag-B438L-II.1R	CATAATCATGATACATTGATTTAAAACATAA	
pMD-Flag-B438L-II.2F	TTATGTTTTAAATCAATGTATCATGATTATG	
pMD-Flag-B438L-II.2R	TAAGAACTACTTATCGTCGTCATCCTTGTAATCCAATGATGGAGATATA GATG	
pMD-Flag-B438L-III.F	CGGATCCGTCGGGCCTTTTTGAAGAATCTTCA	pMD-Flag-B438L-III
pMD-Flag-B438L-III.R	TAAGAACTACTTATCGTCGTCATCCTTGTAATCCAATGATGGAGATATA GATG	
pMD-Flag-tB169L.F	CGGATCCTCCTTTCAAAATCCTTTCATTGTGGC	pMD-Flag-tB169L
pMD-Flag-tB169L.R	GGAATTCTTACTTGTCGTCATCGTCTTTGTAGTCATTATTATATTGAGAAG GC	
pMD-Flag-B169-mATG-2.F	TATTATTTTTGCATTATTGCTTTTTAAATCACCAGTTAA	pMD-Flag-B169-mATG-2
pMD-Flag-tB169-mATG-2.R	TTAACTGGTGATTTAAAACATAATAATGCAAAAATAATA	
qB169L-2-F	TTTGCAATTTGTAATCCGCCGGTG	RT-qPCR for *B169L*-mRNA2
qB169L-2-R	ACTTCTTGTAGGGGTACAAGAGG	

2.3. Construction of Plasmids

The genomic DNA of ASFV was extracted using a MagaBio plus virus DNA purification kit (catalog no. 9109; BioFlux) according to the manufacturer's instructions. Six primer pairs were designed for the amplification of the *B438L-1* to *-6* genes using the genomic DNA as a template. To generate the gene constructs of *B169L-2* and *B169L-mATG-2* (the mutation of the second ATG in *B169L*), a series of reverse primers and intermediate primers were generated and subjected to PCR using the *B438L-1* gene as a template. The mutation and deletion of the GC and TATA boxes in *B438L-7* and *-5* were obtained by sequence overlapping extension (SOE) PCR, and the primers used in this study are shown in Table 1. All the PCR products were purified by using a gel extraction kit (catalog no. 740609.10; TaKaRa) and subsequently digested with the endonucleases *KpnI* and *XhoI*, followed by a second gel purification for subsequent assays. The sequences of the *B438L* promoters were cloned into the pGL3-Basic luciferase reporter plasmid (catalog no. E1751; Promega). The recombinant plasmids were subjected to DNA sequencing.

2.4. Luciferase Reporter Assay

HEK293T cells cultured in 24-well plates were transfected with 0.5 μg of a series of reporter plasmids harboring different *B438L* promoters, a negative control (pGL3-Basic), and a positive control (pGL3-Control) together with 0.05 μg of an internal control plasmid pRL-TK expressing the *Renilla* luciferase.

2.5. Western Blotting Analysis

The HEK293T transfected with the plasmids were lysed with RIPA buffer, and subjected to SDS-PAGE analysis, and then the protein bands were electro-transferred onto nylon membranes. Subsequently, the membranes were blocked in TBS containing 5% skimmed milk for 2 hours at room temperature, and incubated with a mouse anti-Flag monoclonal antibody (MAb) or mouse anti-β-actin polyclonal antibodies (PAb) (catalog no. ZMS1156; Sigma-Aldrich) for 2 hours. The membranes were rinsed three times using TBS containing 0.05% Tween 20 (TBST) and incubated with IRDye 800CW goat anti-mouse IgG secondary antibody (catalog no. 926-32210; LI-COR) for 1 hour at room

 doi:10.20944/preprints202405.0180.v1

temperature. Next, the membranes were scanned using an Odyssey infrared imaging system (LiCor BioSciences).

2.6. RNA Extraction and RT-qPCR

Total RNA was extracted from the PAMs treated with specific inhibitors or virus infection by a Simply P total RNA extraction kit (catalog no. BSC52M1; BioFlux). The isolated RNA was reverse transcribed to cDNA using a FastKing gDNA Dispelling RT SuperMix (catalog no. KR118-02; Tiangen) according to the manufacturer's protocols. The cDNAs were used to analyze the mRNA transcription of *B169L*-2 by RT-qPCR using a QuantStudio system (Applied Biosystems) as described previously [11]. The relative mRNA levels of the target genes were normalized to the internal reference GAPDH, and all primers are listed in Table 1. The relative fold changes in gene expression were determined by the threshold cycle ($2^{-\Delta\Delta CT}$) method [12].

2.7. Statistical Analysis

Statistical analysis was performed using GraphPad Prism 8.0 (San Diego, CA). Statistical differences between groups were assessed by Student's t test. All the experiments were performed independently in triplicates. Error bars represent standard deviations (SD) or standard errors of the mean (SEM) in each group, as indicated in the figure legends (ns, not significant, $P > 0.05$; *, $P < 0.05$; **, $P < 0.01$; ***, $P < 0.001$). A P-value of < 0.05 was considered significant.

3. Results

3.1. Two Distinct Initiation Sites of B438L Transcription

To analyze the transcription start site (TSS) located upstream of the *B438L* translation initiation codon (ATG), 5′RACE assay was conducted using the total RNA of the PAMs infected with the ASFV HLJ/2018 strain at 24 hours postinfection (hpi). The first round of amplification was run by using the B438L-GSP1 primer pairs. The product of the first round of PCR (5 μL) was used as a template to perform the second round of amplification using the B438L-GSP2 primer pairs (Figure 1A). As shown in Figure 1B, PCR products were generated. No PCR products were obtained from the parallel reactions without reverse transcriptase or DNA template (data not shown), indicating that the PCR products were derived from the ASFV transcript. Approximately 20–25 bacterial clones from each 5′RACE product were sequenced and confirmed to harbor an identical 5′-ends, indicating that they were derived from the same *B438L* mRNA transcript. The two positive bands with 700 and 1100 bp, respectively, were mainly amplified by PCR (Figure 1B). Upon sequence alignment, we identified two distinct TSSs located at nt 97563 (TSS-1) and 97848 (TSS-2) of the genome of the ASFV HLJ/2018 strain (Figure 1B). In addition, 3′RACE assay was performed to ascertain the transcription termination site of *B438L*, which was determined to be located at nt 95887 (Figure 1B). Collectively, these findings suggest the presence of two TSSs for the *B438L* gene.

3.2. Identification of the B438L Promoter Region Located in the B169L Gene

To delineate the promoter regions of ASFV *B438L*, a series of primers were designed to amplify seven DNA fragments of the *B438L* gene upstream, using the ASFV genomic DNA as the template (Table 1). Each promoter region was delineated with respect to an individual TSS position, as illustrated in Figure 2A. Notably, these selected promoter regions were designed to lack the ATG codon in the 3′ flanking sequence downstream of the TSS, thereby preventing any potential interference with the translation of the luciferase gene. To evaluate the potential promoter activity of these regions, the DNA fragments were cloned into pGL3-Basic to give rise to the luciferase reporter plasmids.

Subsequently, HEK293T cells were transfected with each the reporter plasmids of different promoter regions and the internal control plasmid pRL-TK for 24 hours. Afterward, the cells were lysed with the passive buffer, and the cell lysates were subjected to the examination of the luciferase

 doi:10.20944/preprints202405.0180.v1

activities using the dual-luciferase reporter assay system according to the manufacturer's instructions. As shown in Figure 2B, all the reporter plasmids did not display any promoter activities. In light of this observation, we presumed that the transcription of the *B438L* gene is likely to depend on ASFV-specific RNA polymerases and other essential transcription factors. To verify the hypothesis, HEK293T cells were transfected with the *B438L* gene reporter plasmids for 12 hours. Subsequently, the cells were infected with an HEK293T cells-adapted ASFV, ASFV-P61 strain [13], at an MOI of 0.1 for 24 hours. Next, the luciferase activities were examined as described above. The results showed that all the reporter plasmids displayed the promoter activities, while the *B438L-1*, *B438L-3*, and *B438L-5* exhibited the higher activities in comparison with *B438L-2*, *B438L-4*, and *B438L-6* (Figure 2C). More specifically, the promoter activities of *B438L-2* and *B438L-4* were shown to be lower than those of *B438L-3* and *B438L-5*, respectively (Figure 2D and E). To further determine whether a promoter exists between *B438L-3* and *B438L-5*, we constructed a luciferase reporter plasmid in the genome region, the data showed that *B438L-7* also exhibited higher activity compared with the negative control (Figure 2F). Taken together, these findings suggest that *B438L-5* and *B438L-7* are responsible for initiating *B438L* transcription at TSS-1 and TSS-2, respectively.

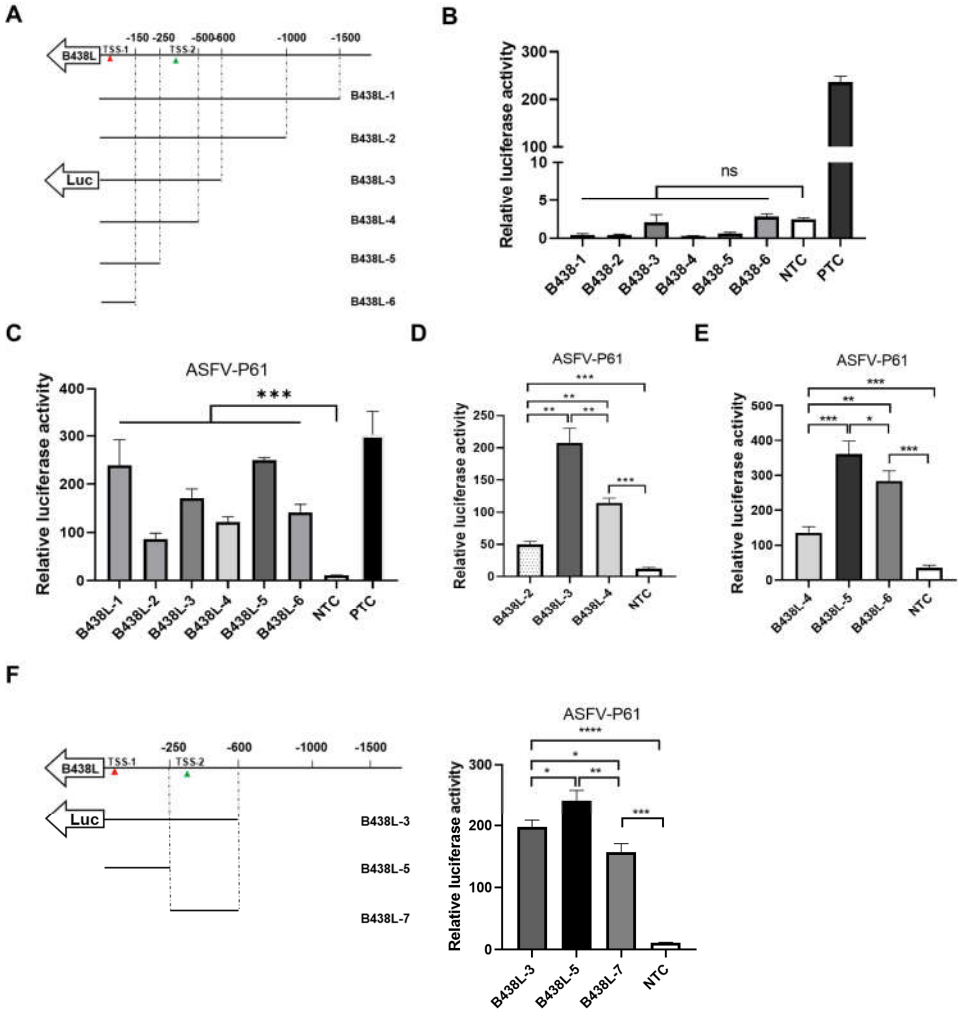

Figure 2. Identification of the *B438L* promoter in the *B169L* gene. (A) Schematic diagram of the *B438L* promoters. Each DNA fragment was obtained by PCR using the primers listed in Table 1. (B) All the promoters of *B438L* did not exhibit promoter activities. HEK293T cells in 6-well plates were transfected with the reporter plasmids (2 μg/each) of *B438L-1* to *-6* for 36 hours, respectively. Subsequently, the cells were lysed and the activities of the *B438L* promoters were analyzed by luciferase reporter assay. (C) *B438L-1*, *-3*, and *-5* exhibited the robust promoter activities upon the ASFV-P61 infection. HEK293T cells were transfected with the reporter plasmids and as described above. Then, the cells were infected with ASFV-P61 strain at a multiplicity of infection of 0.1 for 24

 doi:10.20944/preprints202405.0180.v1

hours. The cells were lysed and subjected to the examination of firefly luciferase and *Renilla* luciferase activities. The data represent the firefly luciferase activity normalized to that of the *Renilla* luciferase. (D and E) The comparison of promoter activities among *B438L-2*, *-3*, and *-4* (D) or *B438L-4*, *-5*, and *-6* (E). (F) The identification of the promoter activity of *B438L-7*. Schematic diagram of the promoters of *B438L-3*, *-5*, and *-7* was shown in the left panel. The promoter activities of *B438L-3*, *-5*, and *-7* were shown in the right panel. All the experiments were performed in triplicates. NTC, negative control, pGL3-Basic; PTC, positive control, pGL3-Control.

3.3. Identification of the TATA and GC Boxes in the B438L Promoter

We have identified two upstream fragments of the *B438L* TSS as promoters. Utilizing a comprehensive analysis of the locations of TATA or GC box within the promoter regions, along with computational analysis [14–17], we have predicted that the putative TATA and GC boxes positioned between 10 and 100 nt, respectively, upstream of TSS (Figure 3A). The TSSs of ASFV-*B438L* were determined at nt 97563 and 97848 in the ASFV HLJ/2018 strain

We predicted its GC and TATA boxes. The primers for amplifying the *B438L* promoter regions are shown in Table 1. The B438L-GSP1 outer and -GSP2 primers were designed based on the genome of ASFV HLJ/2018 strain, while the 5′RACE long and short Universal Primers were provided by the 5′RACE kit. The TATA box or GC box was predicted as described above.

To identify the GC box or TATA box in the regions of *B438L-7* and *B438L-5*, we introduced mutations or deletions (Figure 3B, upper panel) in these cis-acting elements using the mutant primers (Table 1). As shown in Figure 3B, the mutation (*B438L-5*-mGC) or deletion (*B438L-7*-dGC) of the GC box and the mutation of TATA box (*B438L-5*-mTA) resulted in the reduction of the promoter activity. The data indicate that the *B438L* promoters contain functional TATA and GC boxes, which are indispensable for the promoter activity.

To further validate the identified promoter regions, we generated a series of recombinant plasmids expressing *B438L* using the clonal vector pMD-19T, each of which carries one of these two *B438L* promoter regions or two promoter regions. Subsequently, HEK293T cells were transfected with the expressing plasmids of *B438L* ORF with various regions of promoters, pMD-Flag-B438L-I (the region of *B438L-5*), -II (the region of *B438L-7*), and -III (the region of *B438L-3*) or the pMD-19T plasmid, respectively. At 36 hours post transfection (hpt), the cell lysates were analyzed by western blotting to verify the expression of pB438L. Notably, pB438L was efficiently expressed in cells transfected with both plasmids (Figure 3C), indicating that both the distal and proximal promoters of *B438L* can initiate the expression of pB438L.

Preprints.org (www.preprints.org) | NOT PEER-REVIEWED | Posted: 3 May 2024 doi:10.20944/preprints202405.0180.v1

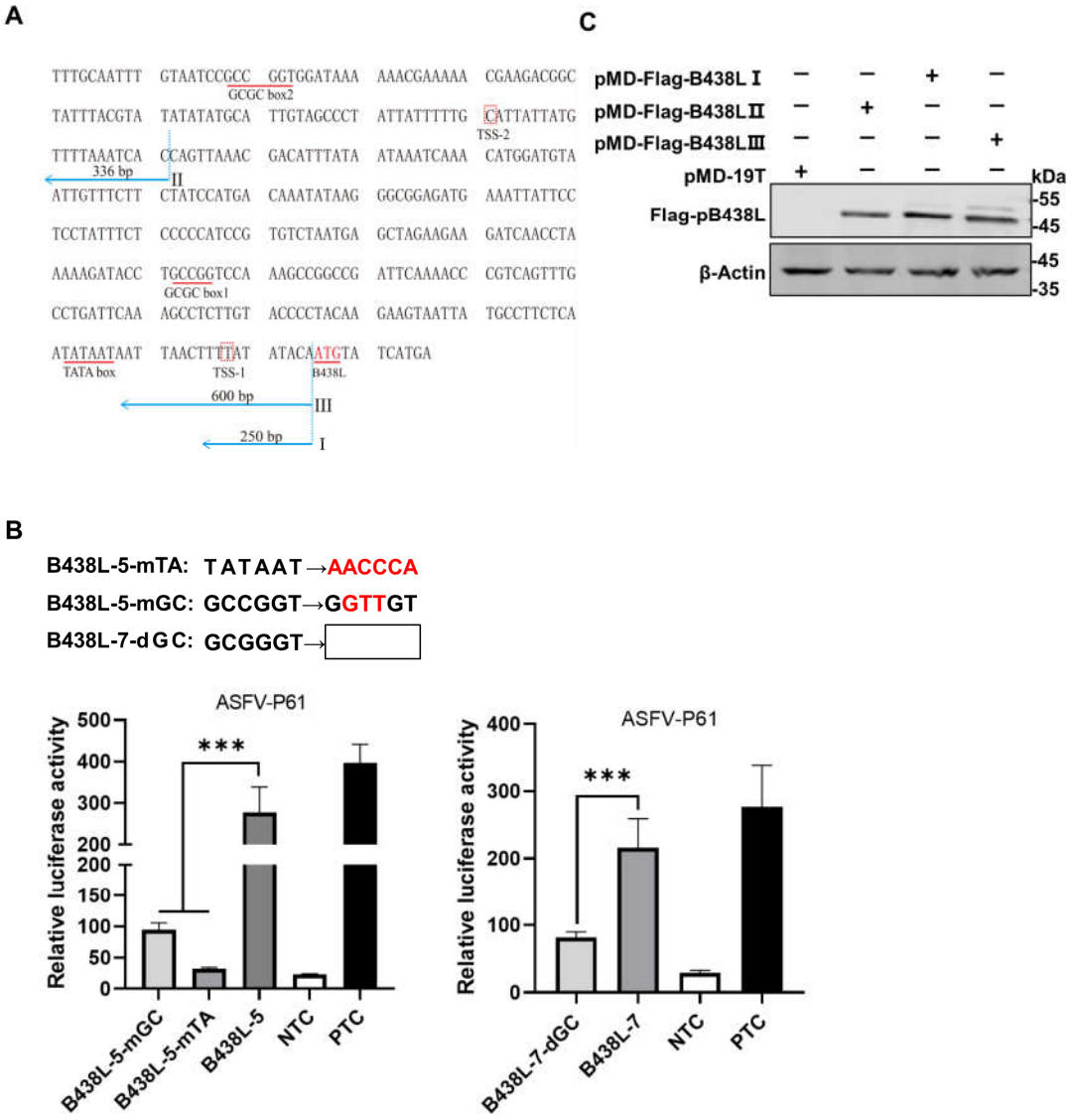

Figure 3. Identification of the TATA and GC boxes in the *B438L* promoter. (A) The predication of TATA and GC boxes in the *B438L* promoter. The TATA and GC boxes were predicted and analyzed by GPMiner (https://bio.tools/GPMiner) and JASPAR (https://jaspar.genereg.net) and Softberry (https://www.softberry.com). The sequences shown in Figure 3A represent the reverse-complement DNA sequences of the promoter regions. The TSSs were examined by 5′RACE and indicated as TSS-1, -2, respectively. (B) The identification of functional TATA and GC boxes in the *B438L* promoter. HEK293T cells in 24-well plates were transfected with the reporter plasmids (2 μg/each) with the mutation or deletion of TATA and GC box of *B438L* promoter, and the cells were infected with ASFV-P61 strain at an MOI of 0.1 for 24 hours. The activities of the *B438L* promoters were determined by luciferase reporter assay. The data represent the firefly luciferase activity normalized to the *Renilla* luciferase activity. The experiments were carried out in triplicates. (C) Both promoter regions (B438L-5, -7) initiate the expression of *B438L*. The plasmids expressing *B438L* under the control of various promoter sequences (2 μg/each), i.e., pMD-Flag-B438L-I (*B438L-5*, the region of nt 97555~97804), -II (*B438L-7*, the region of nt 97819~98154) or -III (*B438L-3*, the region of nt 97555~98154) or the empty vector pMD-19T, were transfected into HEK293T cells for 24 hours. Then the cells were infected with the ASFV-P61 strain as described above. Subsequently, the immunoblotting analyses were performed with an anti-Flag monoclonal antibody. NTC, negative control, pGL3-Basic; PTC, positive control, pGL3-Control.

 doi:10.20944/preprints202405.0180.v1

3.4. Identification of the B438L Distal Promoter that Initiates Transcription of B169L-2

Since the *B438L* distal promoter is located in the *B169L* gene, we investigate whether the promoter affects the *B169L* expression. To this end, we reviewed the relevant data and found that there is *B169L*-mRNA2 encoding a truncated pB169L (tpB169L) (amino acids 92–169). The sequence of *B169L-2* is located in the downstream of the *B438L* distal promoter. Thus, we verified whether the *B438L* distal promoter is capable of initiating the transcription of *B169L-2*. Firstly, we constructed the recombinant plasmid pMD-Flag-tB169L, which carries the gene sequence of *B169L-2* as well as the distal promoter sequence of *B438L*. Secondly, HEK293T cells were transfected with pMD-Flag-tB169L or pMD-Flag-B438L-II and infected with ASFV-P61. At 24 hpi, the cell lysates were analyzed by western blotting to verify the expression of tpB169. Notably, tpB169L was expressed in the pMD-Flag-tB169L-transfected HEK293T cells (Figure 4A), indicating that the distal promoter of *B438L* can initiate the expression of tpB169L.

We further analyzed the sequences of *B169L-2* and revealed that the gene contains two initiation codon (ATG-2 and ATG-3) located in the region between TSS-2 and the termination codon TAA-1 (Figure 4A). Further study demonstrated that there is a termination codon (TAA-2) located in the 15 nt downstream of ATG-2, and ATG-3 is required for the translation of *B169L*-2. We speculated that the transcription efficiency of *B169L-2* was impaired due to the presence of a mini transcript (located in the region of ATG-2 and TAA-2). Thus, we mutated the ATG-2 of *B169L* and constructed the Flag-tagged mutant plasmid pMD-B169L-mATG-2. Next, HEK293T cells were transfected with pMD-tB169L, pMD-B169L-mATG-2 and infected with ASFV-P61. At 24 hpi, cell lysates were collected to examine the protein expression of pMD-Flag-tB169L and pMD-tB169L-mATG2 by western blotting, and total RNA was extracted for reverse transcription-quantitative PCR (RT-qPCR) to determine the mRNA transcription. The results showed that the transcription and translation efficiency of pMD-tB169L-mATG2 were significantly higher than that of pMD-Flag-tB169L (Figure 4B and C), indicating that the *B438L* distal promoter is capable of initiating the transcription of *B438L* as well as *B169L-2*, and that the mutation of the ATG-2 located between the TSS-2 of *B438L* and the ATG of *B169L-2* (ATG-3) can efficiently enhance the expression of *B169L-2*.

 doi:10.20944/preprints202405.0180.v1

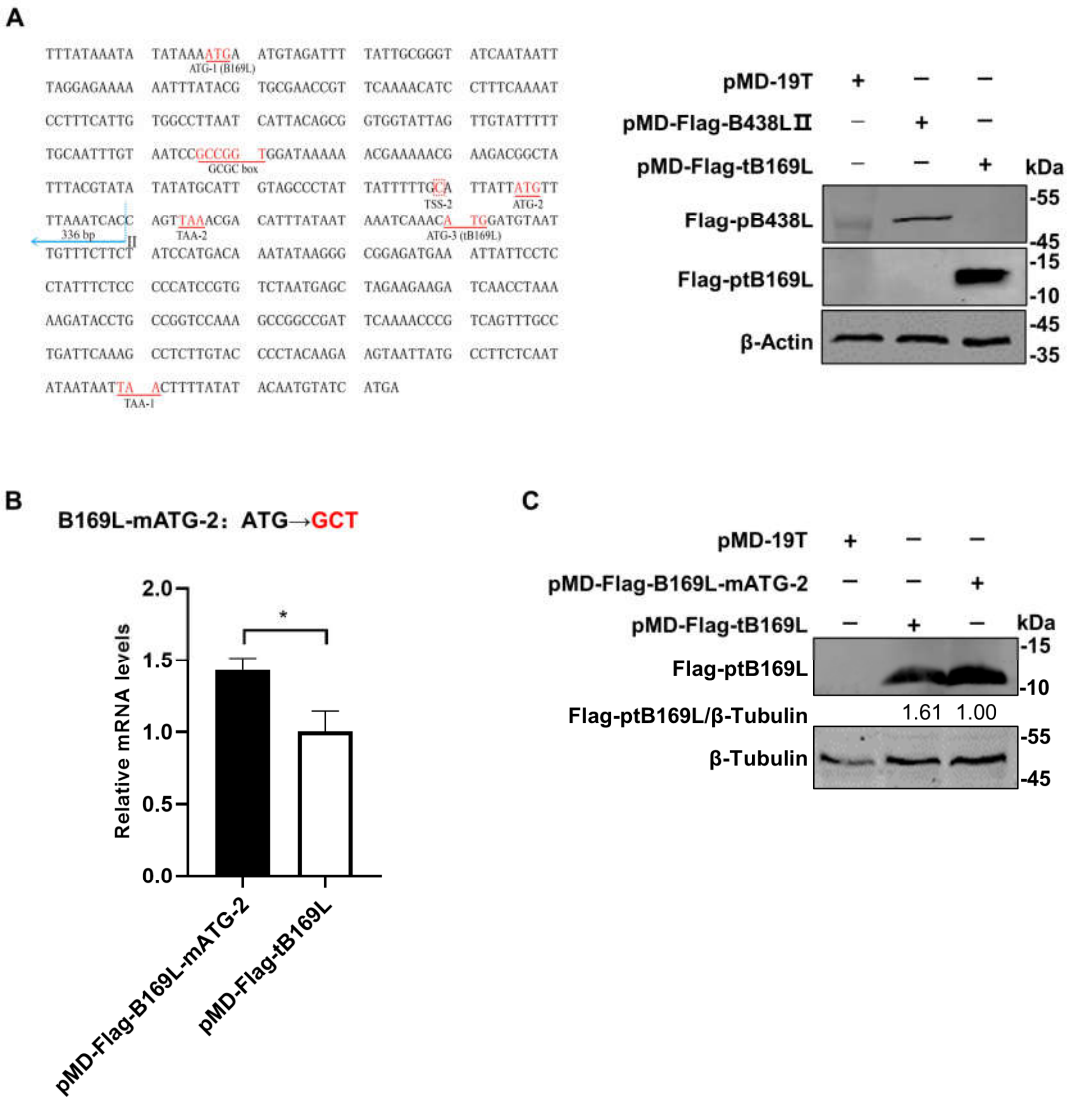

Figure 4. Identification of the *B438L* promoter that initiates the transcription of *B169L-2*. (A) The *B438L* distal promoter is capable of initiating the transcription of *B169L-2*. HEK293T cells in 6-well plates were transfected with pMD-Flag-tB169L or pMD-Flag-B438L-II (2 μg/each), followed by infection with ASFV-P61 strain as described above. Subsequently, the immunoblotting analysis was performed with an anti-Flag monoclonal antibody (MAb). The sequences shown in Figure 4A (left panel) represent the reverse-complement DNA sequences of the promoter regions. (B and C) The *B169L-2* transcription efficiency is affected by the second initiation codon (ATG-2). HEK293T cells were transfected with pMD-Flag-tB169L or pMD-Flag-B169L-mATG-2 (2 μg/each) and infected with the ASFV-P61 strain as described above. Subsequently, the transcription level of *B169L-2* was measured by relative reverse transcription-quantitative PCR (B), and the protein expression of ptB169L (encoding by *B169L*-mRNA2) was analyzed by immunoblotting analysis using the anti-Flag MAb (C).

4. Discussion

Viruses have evolved multiple strategies to regulate the viral gene expression to complete the virus life cycle. Multiple promoters enable viruses to selectively activate or repress genes depending on different cell types, microenvironment, or the stages of the virus life cycle, thereby enhancing viral adaptation in host cells. For example, the HIV-1 *Nef* gene contains multiple promoters, each of which plays a different regulatory role in different cell types and conditions [18,19].

In this study, we revealed that two promoter regions responsible for the ASFV *B438L* transcription located upstream of the *B438L* ORF. In addition, we demonstrate the *B169L* gene (the upstream gene of *B438L*) contains a distal promoter for *B438L*. Interestingly, this distal promoter not

 doi:10.20944/preprints202405.0180.v1

only initiates the transcription of the *B438L* gene but also governs the transcription of *B169L-2*, suggesting the precise regulatory association of the adjacent viral genes.

Furthermore, we have also observed an initiation codon (ATG-2) located upstream of *B169L-2* (Figure 4A). Unexpectedly, substitution of the ATG with GCT resulted in an enhanced transcription and translation efficiency for *B169L-2* (Figure 4B). The presence of the ATG-2 is likely to be involved in modulating the expression of the downstream *B169L-2*, while the mutation of ATG-2 is speculated to abolish the binding between transcription factors and the promoter, thereby releasing the transcription factors for favoring the downstream gene transcription. Besides, in the absence of viral infection, all of the luciferase reporter plasmids were devoid of promoter activity. In contrast, in the presence of viral infection, all of the luciferase reporter plasmids exhibited the promoter activities, suggesting that regulation of these two promoters requires the participation of the ASFV-encoded polymerases and their associated factors. Here, we identified for the first time the transcriptional regulatory element for *B169L-2*, indicating that ASFV employs multiple strategies to regulate gene expression. Future studies are required to investigate the functional role of *B169L-2* during ASFV replication. Furthermore, the findings will facilitate the design of the *B169L* gene-deleted ASFV. The phenomenon of multiple promoters regulating the transcription of viral genes is an interesting topic in virology.

Additionally, multiple promoters enhance viral adaptation to host diversity, exhibiting the distinct biological characteristics. It has been shown that the *X* gene of hepatitis B virus (HBV) contains multiple promoters, therefore, regulating gene expression under different conditions [20,21]. Viruses also utilize multiple promoters to regulate gene expression patterns for the immune evasion of host cells. The herpes simplex virus 1 (HSV-1) *UL34* gene (ICP0) contains multiple promoters, which functions at multiple stages of the virus life cycle [22,23].

Moreover, the presence of multiple promoters contributes to the genetic diversity of viral genes, thereby facilitating immune-evasion of host cells. The *IE1* gene of human cytomegalovirus (CMV) has multiple promoters, with these promoters playing a pivotal role in viral infection, enhancing our understanding of CMV gene regulation [24,25]. Finally, different promoters are activated during various stages of the viral life cycle, favoring virus replication and transmission. The *LMP1* gene of Epstein-Barr virus (EBV) contains multiple promoters, resulting in the expression of various LMP1 proteins, which are crucial for comprehending the complex regulatory network of EBV [26,27]. Taken together, we demonstrated that the distal promoter of *B438L* gene initiates the transcription of both the *B438L* mRNA and *B169L* mRNA2.

5. Conclusions

In conclusion, we demonstrated for the first time that the ORF of the ASFV *B438L* gene was governed by two different promoters, and the distal promoter could also initiate the transcription of both *B438L* and *B169L-2* genes (Figure 5). A comprehensive understanding of the multiple promoters of viral genes can facilitate the development of more effective antiviral strategies.

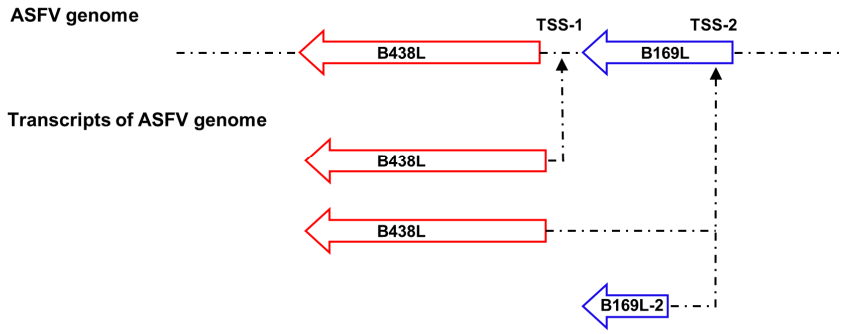

Figure 5. A working model for the transcription of the *B438L* and *B169L-2* genes of ASFV. The *B438L* gene was governed by two different promoters, and the distal promoter could also initiate the transcription of both the *B438L* and *B169L-2* genes.

Author Contributions: Conceptualization, H.C., H.D., and Y.W.; methodology, H.C., H.D., and Y.W.; software, H.C., H.D., and D.L.; validation, H.C., H.D., and Y.W.; formal analysis, H.C., M.L., and L.L.; investigation, H.C.; resources, H.Q.; data curation, S.L.; writing—original draft preparation, H.C.; writing—review and editing, H.Q., and S.L; visualization, D.P., J.D., and J.J.; supervision, S.L.; project administration, H.Q.; funding acquisition, H.Q., and S.L. All authors have read and agreed to the published version of the manuscript.".

Funding: This work was supported by the Natural Science Foundation of China (grants 32072866 and U20A2060), and the Heilongjiang Provincial Natural Science Foundation of China (grant YQ2022C043).

Informed Consent Statement: Not applicable.

Data Availability Statement: Data supporting the reported results are available in this article.

Conflicts of Interest: The authors declare no conflict of interest in this work.

References

1. Iyer, L.M.; Aravind, L.; Koonin, E.V. Common origin of four diverse families of large eukaryotic DNA viruses. *J. Virol*. **2001**, *75*, 11720–11734.
2. Alejo, A.; Andrés, G.; Salas, M.L. African swine fever virus proteinase is essential for core maturation and infectivity. *J. Virol*. **2003**, *77*, 5571–5577.
3. Carrascosa, A.L.; Bustos, M.J.; de Leon, P. Methods for growing and titrating African swine fever virus: field and laboratory samples. *Curr. Protoc. Cell Biol*. **2011**, *26*, 21–26.
4. Chen, W.; Zhao, D.; He, X.; Liu, R.; Wang, Z.; Zhang, X.; Li, F.; Shan, D.; Chen, H.; Zhang, J.; et al. A seven-gene-deleted African swine fever virus is safe and effective as a live attenuated vaccine in pigs. *Sci. China Life Sci*. **2020**, *63*, 623–634.
5. Dixon, L.K.; Chapman, D.A.; Netherton, C.L.; Upton, C. African swine fever virus replication and genomics. *Virus Res*. **2013**, *173*, 3–14.
6. Cackett, G.; Matelska, D.; Sýkora, M.; Portugal, R.; Malecki, M.; Bähler, J.; Dixon, L.; Werner, F. The African swine fever virus transcriptome. *J. Virol*. **2020**, *94*, e00119-20
7. Epifano, C.; Krijnse-Locker, J.; Salas, M.L.; Salas, J.; Rodríguez, J.M. Generation of filamentous instead of icosahedral particles by repression of African swine fever virus structural protein pB438L. *J. Virol*. **2006**, *80*, 11456–11466.
8. Zhan, Y.; Zhang, L.H.; Lin, Y.; Cai, Y.F.; Zou, Y.W.; Hao, Z.Y.; Luo, Z.H.; Wang, N.D.; Deng, Z.B.; Yang, Y.; et al. Development and preliminary testing of a probe-based duplex real-time PCR assay for the detection of African swine fever virus. *Mol. Cell*. **2021**, *Probes 59*, 101764.
9. Cackett, G.; Sýkora, M.; Werner, F. Transcriptome view of a killer: African swine fever virus. *Biochem. Soc. Trans*. **2020**, *48*, 1569-1581.
10. Zhao, D.; Liu, R.; Zhang, X.; Li, F.; Wang, J.; Zhang, J.; Liu, X.; Wang, L.; Zhang, J.; Wu, X.; et al. Replication and virulence in pigs of the first African swine fever virus isolated in China. *Emerg. Microbes Infect*. **2019**, *8*, 438–447.
11. Zhou, P.; Li, L.F.; Zhang, K.; Wang, B.; Tang, L.; Li, M.; Wang, T.; Sun, Y.; Li, S.; Qiu, H.J. Deletion of the H240R gene of African swine fever virus decreases infectious progeny virus production due to aberrant virion morphogenesis and enhances inflammatory cytokine expression in porcine macrophages. *J. Virol*. **2022**, *96*, e0166721.
12. Livak, K.J.; Schmittgen, T.D. Analysis of relative gene expression data using real-time quantitative PCR and the 2-ΔΔCT Method. *Methods* **2001**, *25*, 402–408.
13. Wang, T.; Sun, Y.; Huang, S.; Qiu, H.J. Multifaceted immune responses to African swine fever virus: implications for vaccine development. *Vet. Microbiol*. **2020**, *249*, 108832.
14. Lee, T.Y.; Chang, W.C.; Hsu, J.B.; Chang, T.H.; Shien, D.M. GPMiner: an integrated system for mining combinatorial cis-regulatory elements in mammalian gene group. *BMC. Genomics*. **2012**, *13 Suppl 1*, S3.
15. Shrivastava, S.; Bhanja C.J.; Steele, R.; Ray, R.; Ray, R.B. Hepatitis C virus upregulates Beclin1 for induction of autophagy and activates mTOR signaling. *J. Virol.* **2012**, *86*, 8705–8712.
16. Smale, S.T.; Kadonaga, J.T. The RNA polymerase II core promoter. *Annu. Rev. Biochem*. 2003, *72*, 449–479.
17. Wasserman, W.W.; Sandelin, A. Applied bioinformatics for the identification of regulatory elements. *Nat. Rev. Genet*. **2004**, *5*, 276–287.
18. Furtado, M.R.; Balachandran, R.; Gupta, P.; Wolinsky, S.M. Analysis of alternatively spliced human immunodeficiency virus type-1 mRNA species, one of which encodes a novel tat-env fusion protein. *Virology* **1991**, *185*, 258–270.
19. Telwatte, S.; Lee, S.; Somsouk, M.; Hatano, H.; Baker, C.; Kaiser, P.; Kim, P.; Chen, T.H.; Milush, J.; Hunt, P.W.; et al. Gut and blood differ in constitutive blocks to HIV transcription, suggesting tissue-specific differences in the mechanisms that govern HIV latency. *PLoS Pathog*. **2018**, *14*, e1007357.
20. Shimoda, A.; Sugata, F.; Chen, H.S.; Miller, R.H.; Purcell, R.H. Evidence for a bidirectional promoter complex within the X gene of woodchuck hepatitis virus. *Virus Res*. **1998**, *56*, 25–39.

 doi:10.20944/preprints202405.0180.v1

21. Slagle, B.L.; Bouchard, M.J. Hepatitis B virus *X* and regulation of viral gene expression. *Cold Spring Harb. Perspect. Med*. **2016**, *6*, a021402.
22. Kawaguchi, Y.; Tanaka, M.; Yokoymama, A.; Matsuda, G.; Kato, K.; Kagawa, H.; Hirai, K.; Roizman, B. Herpes simplex virus 1 alpha regulatory protein ICP0 functionally interacts with cellular transcription factor BMAL1. *Proc. Natl. Acad. Sci. U. S. A.* **2001**, *98*, 1877–1882.
23. Wijesekera, N.; Hazell, N.; Jones, C. Independent cis-regulatory modules within the herpes simplex virus 1 infected cell protein 0 (ICP0) promoter are transactivated by Krüppel-like factor 15 and glucocorticoid receptor. *Viruses* **2022**, *14*, 1284.
24. Jeang, K.T.; Rawlins, D.R.; Rosenfeld, P.J.; Shero, J.H.; Kelly, T.J.; Hayward, G.S. Multiple tandemly repeated binding sites for cellular nuclear factor 1 that surround the major immediate-early promoters of simian and human cytomegalovirus. *J. Virol.* **1987**, *61*, 1559–1570.
25. Stinski, M.F.; Isomura, H. Role of the cytomegalovirus major immediate early enhancer in acute infection and reactivation from latency. *Med. Microbiol*. **2008**, *197*, 223–231.
26. Pai, S.; Khanna, R. Role of LMP1 in immune control of EBV infection. *Semin. Cancer Biol*. **2001**, *11*, 455–460.
27. Ryan, J.L.; Morgan, D.R.; Dominguez, R.L.; Thorne, L.B.; Elmore, S.H.; Mino-Kenudson, M.; Lauwers, G.Y.; Booker, J.K.; Gulley, M.L. High levels of Epstein-Barr virus DNA in latently infected gastric adenocarcinoma. *Lab. Invest*. **2009**, *89*, 80–90.